Attractive, weakly attractive, and repulsive near-critical systems

Pablo G. Debenedetti and Rahoma S. Mohamed

Department of Chemical Engineering, Princeton University, Princeton, New Jersey 08544

Mixtures composed of trace amounts of a solute in the vicinity of a solvent's critical point exhibit one of three types of behavior: repulsive, weakly attractive, or attractive. Each regime is characterized by the signs of the diverging solute partial molar volume (and enthalpy), and of the correlations between solute and solvent concentration fluctuations at infinite dilution. Attractive behavior, in which the former quantity is negative and the latter positive, underlies all of the actual or proposed applications of supercritical fluids to processes ranging from precipitation polymerization to activated carbon regeneration. The presence of trace amounts of a solute within a solvent characterized by long-ranged density fluctuations gives rise to a cooperative phenomenon which, for attractive systems, involves the formation of a large solvent-rich region around each solute molecule. Likewise, for repulsive behavior, the cooperative phenomenon involves the formation of a large solvent-deficient region around each solute molecule. The calculated volume, enthalpy, and entropy changes per solvent molecule are very similar to the corresponding condensation (attractive behavior) and evaporation (repulsive behavior) effects for the pure solvent at subcritical temperatures. This suggests a qualitative description of near-critical cooperative phenomena as induced phase transitions.

INTRODUCTION

In recent years, several experimental studies have addressed the nature of solvent–solvent interactions in very dilute mixtures in the vicinity of solvent critical points.[1-4] Using techniques ranging from density measurements[1,2] in experiments aimed at studying solute partial molar volumes, to solvatochromic probes[3,4] in investigations of local compositions around solute molecules, these studies have allowed the observation and quantification of theoretically predicted phenomena, such as large negative solute partial molar volumes,[5-7] and solvent enrichment around solute molecules.[8]

The thermodynamics of mixtures composed of trace amounts of a solute in the vicinity of a solvent's critical point (near-critical mixtures) was first studied by Krichevskii and his colleagues[6,9] using classical arguments. These workers showed that solute partial molar volumes, energies, and enthalpies diverge at the solvent's critical point (divergence), whereas the corresponding solvent properties attain finite limits, the value of which depends upon the path along which the critical point is approached (path dependence). The nonclassical analysis of this problem was pioneered by Wheeler,[10] in his elegant decorated lattice[11-13] treatment of near-critical thermodynamics. Recent contributions include the work of Levelt Sengers and co-workers,[14-21] and that of Gilbert and Eckert.[22]

In the vicinity of the critical point of any substance, the length over which density fluctuations are correlated becomes arbitrarily large. For attractive solute–solvent interactions, the presence of a solute in trace amounts gives rise to a cooperative phenomenon involving the "condensation" of an arbitrarily large amount of solvent molecules (clustering). The experimentally measured large negative solute partial molar volumes in infinitely dilute mixtures of nonvo-

latile solids in supercritical fluids[1,2] are macroscopically measurable manifestations of clustering. Positively diverging solute partial molar volumes at infinite dilution,[23] on the other hand, are macroscopically measurable consequences of the presence of trace amounts of a solute within a medium characterized by a diverging correlation length, when solute–solvent interactions are repulsive.

In two recent publications[8,24] we have quantified these cooperative phenomena. Specifically, we defined a cluster size as the excess number of solvent molecules surrounding the infinitely dilute solute, with respect to a uniform distribution at bulk conditions. This quantity, which can be either positive or negative, is proportional to the solvent's compressibility, and hence is very large in magnitude in the near-critical region. Because the diverging partial molar quantities are also proportional to the solvent's compressibility,[10,24] the cooperative enthalpy, volume, and entropy changes per solvent molecule are necessarily finite. In this paper we investigate the magnitude of these effects. The entropy, enthalpy, and volume changes are indicative of an induced condensation (attractive interactions) or evaporation (repulsive solute–solvent interactions) around the solute molecule.

Near-critical systems can be of three types: repulsive, weakly attractive, and attractive. These are characterized by the signs of the diverging solute partial molar volume and of the cluster size, which can be either (+ , −), (+ , +), or (− , +), respectively. The three types of behavior can be derived both from continuum and microscopic models. Here, we compare the similarities and differences between the picture of near-critical mixtures that emerges from the van der Waals model and from Wheeler's decorated lattice treatment. Significant differences arise between these models as to the predicted behavior of the symmetrical near-

critical system obtained by interchanging solute and solvent.

The behavior of a mixture at infinite dilution and near-critical conditions is not only scientifically but also technologically relevant. In fact, the phase behavior exhibited by most systems used in actual or proposed applications of supercritical fluids is largely determined by the attractive nature of the mixtures involved. In these processes, which include coffee decaffeination,[25] enhanced oil recovery,[26] and precipitation polymerization,[27,28] a nonvolatile solute is contacted with a supercritical fluid to form a dilute solution in which solute properties are not too different from their infinite dilution values. Both the experimentally observed solubility enhancements of up to six orders of magnitude with respect to ideal gas behavior, and the exothermic dissolution of the pure solid solutes into the supercritical fluid, two key features of dilute supercritical mixtures of practical interest, have been shown to be a direct consequence of the attractive behavior of these systems at infinite dilution.[8,24]

In what follows we derive van der Waals and decorated lattice criteria for the classification of near-critical mixtures, we show the similarities and differences between the two approaches, we quantify the entropy, enthalpy, and volume effects which accompany the isothermal, isobaric addition of trace amounts of a solute to a near-critical solvent, and we show the analogies and differences between these cooperative phenomena and first-order phase transitions.

ATTRACTIVE, WEAKLY ATTRACTIVE, AND REPULSIVE SYSTEMS

The partial molar volume of an infinitely dilute solute (1) in a binary mixture (1,2) is given by the identity

$$\overline{V}_1^\infty = \rho^{-1} K_T \left[\left(\frac{\partial P}{\partial N_1} \right)_{T,V,N_2} \cdot N \right]^\infty \equiv \rho^{-1} K_T \delta, \qquad (1)$$

where superscript ∞ denotes the limit of vanishing solute–solute interactions, ρ and K_T are the solvent's number density and isothermal compressibility, and N, the total number of molecules in a volume V. The quantity in brackets (δ), which at infinite dilution can also be written as

$$\delta = \left(\frac{\partial P}{\partial x_1} \right)_{T,\rho}^\infty + K_T^{-1}, \qquad (2)$$

where x_1 is a molecule fraction, is finite arbitrarily close to the solvent's critical point.[5,10] We define the cluster size ξ (not to be confused with the correlation length, for which the same symbol is frequently used), as the excess number of solvent molecules surrounding an infinitely dilute solute molecule, with respect to a uniform distribution at the prevailing bulk density,[8,24,29]

$$\xi = \rho \int (g_{21}^\infty - 1) d^3 r = \lim_{x_1 \to 0} \frac{\langle \delta N_1 \delta N_2 \rangle}{\langle N_1 \rangle}, \qquad (3)$$

where ρ is the solvent's number density, g_{21}^∞, the infinite dilution limit of the unlike pair correlation function, δN_i, an instantaneous fluctuation in the number of molecules of type i within an open control volume containing, on average, $\langle N_1 \rangle$ noninteracting solute molecules, and $\langle \ \rangle$ denotes thermodynamic averaging. Note that ξ can be either positive or negative.

A relationship between ξ and $\overline{V}_1^\infty$ can be obtained from the theory of fluctuations.[29] The result is[8]

$$\overline{V}_1^\infty \rho = \rho k T K_T - \xi \qquad (4)$$

or equivalently, using Eq. (1)

$$\overline{V}_1^\infty \rho \xi^{-1} = \frac{\delta}{\rho k T - \delta} \qquad (5)$$

In the vicinity of the solvent's critical point, $\overline{V}_1^\infty$ and ξ diverge strongly (i.e., as K_T), their signs being those of δ and $\rho k T - \delta$, respectively. The unbounded growth of ξ, a direct consequence of the divergence of the correlation length, endows this otherwise purely statistical quantity with mechanistic significance.[8,24] The proportionality between $\overline{V}_1^\infty$ and ξ means that, except for the special case $\rho k T \approx \delta$ (to be discussed below), the ratio $\overline{V}_1^\infty \xi^{-1}$ is finite. Along the critical isochore, in particular,

$$\overline{V}_1^\infty \xi^{-1} \rho_c = \frac{\delta}{\rho_c k T - \delta} \equiv \phi, \qquad (6)$$

where ρ_c is the solvent's critical density, and it is understood that δ is evaluated at T and ρ_c. The quantity ϕ is the volume change associated with cluster formation (in units of ρ_c^{-1}) per solvent molecule in the cluster (i.e., per excess solvent molecule surrounding the infinitely dilute solute, with respect to a uniform distribution at the prevailing density).

We now discuss the behavior of δ and $\rho k T - \delta$. In particular, we seek to compare the signs of these quantities in the near-critical region as predicted by a nonclassical and microscopic model with the corresponding predictions according to a classical and continuum model. In the former case, we invoke Wheeler's decorated lattice treatment of infinitely dilute near-critical behavior,[10] and write

$$\rho^{-1} \delta = \frac{kT\{(1 - (x-1)^2[N' - (\partial N'/\partial \ln \rho)_T]\}}{1 + (x^2 - 1)\rho - N'(x-1)^2}, \qquad (7)$$

where N' is the number of empty–filled nearest-neighbor contacts in the primary lattice (normalized by the number of primary cells times the coordination number), ρ is a dimensionless solvent density (i.e., the ratio of solvent molecules to the total number of cells in the primary lattice), and

$$x = \exp(-\epsilon_{12}/kT), \qquad (8)$$

where ϵ_{12} is the solute–solvent interaction energy. In this model, ϵ_{12} can be either positive (repulsive solute–solvent interactions) or negative (attractive interactions). Note that, since ρ is dimensionless in Eq. (7), δ has units of energy and differs from the quantity defined in Eq. (1) by the trivial factor v_0 (the volume of a unit cell in the primary lattice). The partial derivative $\partial N'/\partial \rho$ vanishes at the critical point, and N' approaches a limiting value (N_c) between $\cdot 17$ and $\cdot 19$ in three-dimensional lattices.[10] As shown in the Appendix, Eq. (7) implies, at the critical point, the following criteria for the signs of the diverging quantities ($\overline{V}_1^\infty$ and ξ).

$$\overline{V}_1^\infty > 0 \quad (\text{i.e., } \delta > 0) \text{ for } \epsilon_{12}/kT > -\ln(1 + N_c^{-1/2}), \qquad (9a)$$

$$\overline{V}_1^\infty < 0 \quad (\text{i.e., } \delta < 0) \text{ for } \epsilon_{12}/kT < -\ln(1 + N_c^{-1/2}), \qquad (9b)$$

$\xi > 0$ (i.e., $\rho kT - \delta > 0$) for $\epsilon_{12} < 0$,   (10a)

$\xi < 0$ (i.e., $\rho kT - \delta < 0$) for $\epsilon_{12} > 0$.   (10b)

In the vicinity of the critical point Eqs. (9a) and (9b) are formally identical, but with N_c replaced by $[N' - \partial N'/\partial \ln \rho]$, an inconsequential change, since $N' \approx N_c$ and $\partial N'/\partial \ln \rho \approx 0$. Equations (10a) and (10b) are unchanged away from the critical point for $|\partial N'/\partial \rho| < 1$ (see the Appendix).

The above regimes are summarized in Fig. 1. A near-critical mixture is repulsive when $\overline{V}_1^\infty > 0$ and $\xi < 0$ ($\epsilon_{12} > 0$), weakly attractive if $\overline{V}_1^\infty > 0$ and $\xi > 0 [-\ln(1 + N_c^{-.5}) < \epsilon_{12}/kT < 0]$, and attractive if $\overline{V}_1^\infty < 0$ and $\xi > 0$ $[\epsilon_{12}/kT < -\ln(1 + N_c^{-.5})]$. Regimes analogous to those shown in Fig. 1, but with a characteristic function of solute and solvent concentration fluctuations at infinite dilution as a parameter (instead of ϵ_{12}/kT) were recently derived[8] in conjunction with Eq. (4).

The correlation length for density fluctuations diverges at the critical point of any pure substance. The presence of trace amounts of a solute in a near-critical fluid gives rise to a cooperative phenomenon involving participation of an arbitrarily large number of solvent molecules (ξ). For repulsive solute–solvent interactions ($\delta > \rho kT$), ξ is large and negative in the near-critical region. Each solute molecule is then surrounded by a solvent-deficient region, the characteristic size of which is the correlation length. The resulting volume expansion is reflected in the sign of $\overline{V}_1^\infty$. For attractive systems ($\delta < 0$), a solvent-rich region of characteristic size equal to the correlation length surrounds solute molecules (ξ large and positive, $\overline{V}_1^\infty$ large and negative). If the solute–solvent interactions are weakly attractive ($0 < \delta < \rho kT$), positive solute–solvent correlations ($\xi > 0$) coexist with positively diverging partial molar volumes. This behavior can be explained through the following thought experiment. Imagine a pure solvent, to which trace amounts of a solute are added isobarically and isothermally. Let the solute be infinitely smaller than the solvent, and let its interactions with the solvent be vanishingly weak. In this case, obviously, $\xi \to 0$. Even for such a "transparent" solute, $\overline{V}_1^\infty$ becomes large and positive in the near-critical region, owing to the divergence of K_T [see Eq. (4)]. Real solutes which interact attractively with the solvent ($\xi > 0$) must first overcome this purely osmotic effect before $\overline{V}_1^\infty$ can become negative. Weakly attractive systems are therefore those in which clustering is insufficient to overcome the osmotic volume change due to solute addition, namely, kTK_T.[30]
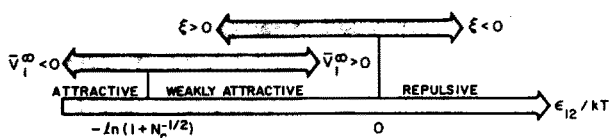
In Wheeler's model, then, the classification of a near-critical system into attractive, weakly attractive, or repulsive is expressed entirely in terms of the solute–solvent interaction energy. We now compare these predictions with those of a classical and continuum model, the van der Waals mixture $[P = \rho kT(1 - \rho b)^{-1} - a\rho^2]$. In this case, we have

$$\delta = \frac{\rho kT}{(1 - \rho b)^2} [1 + \rho(b_1 - b_2)] - 2\rho^2 a_{12},   (11)$$

where $b = \Sigma x_i b_i$, and $a = \Sigma\Sigma x_i x_j a_{ij}$. Along the critical isochore (ρ_c), Eq. (11) implies

$$\overline{V}_1^\infty > 0   \text{(i.e., } \delta > 0) \text{ for } \gamma > \frac{3\alpha^{1/2}}{T_r} - 2,   (12a)$$

$$\overline{V}_1^\infty < 0   \text{(i.e., } \delta < 0) \text{ for } \gamma < \frac{3\alpha^{1/2}}{T_r} - 2,   (12b)$$

$$\xi > 0   \text{(i.e., } \rho kT - \delta > 0) \text{ for } \gamma < \frac{3\alpha^{1/2}}{T_r} - \frac{2}{3},   (13a)$$

$$\xi < 0   \text{(i.e., } \rho kT - \delta < 0) \text{ for } \gamma > \frac{3\alpha^{1/2}}{T_r} - \frac{2}{3},   (13b)$$

where $T_r \equiv T/T_c$, and

$$\alpha = a_{11}/a_{22},   (14)$$

$$\gamma = b_1/b_2,   (15)$$

and where $a_{12} = (a_{11}a_{22})^{1/2}$.

A near-critical van der Waals mixture, then, is repulsive when $\overline{V}_1^\infty > 0$ and $\xi < 0 (\gamma > 3\alpha^{1/2}/T_r - 2/3)$, weakly attractive if $\overline{V}_1^\infty > 0$ and $\xi > 0$ $(3\alpha^{1/2}/T_r - 2 < \gamma < 3\alpha^{1/2}/T_r - 2/3)$, and attractive if $\overline{V}_1^\infty < 0$ and $\xi > 0$ $(\gamma < 3\alpha^{1/2}/T_r - 2)$. These regimes are illustrated in Fig. 2, which also includes $(\alpha^{1/2}, \gamma)$ coordinates corresponding to several systems for which large positive $(+)$ and negative $(-)$ solute partial molar volumes have been measured[2,23,31] in the near-critical region. The discrep-

FIG. 1. The three possible types of behavior which characterize a near-critical mixture, according to Wheeler's decorated lattice model.[10] Attractive behavior (ϵ_{12} large and negative) implies volume contraction upon isobaric solute addition and solvent enrichment around the solute. Repulsive behavior (ϵ_{12} positive) implies volume expansion upon isobaric solute addition, and solvent depletion around the solute. Weakly attractive behavior (ϵ_{12} small and negative) implies volume expansion and solvent enrichment.
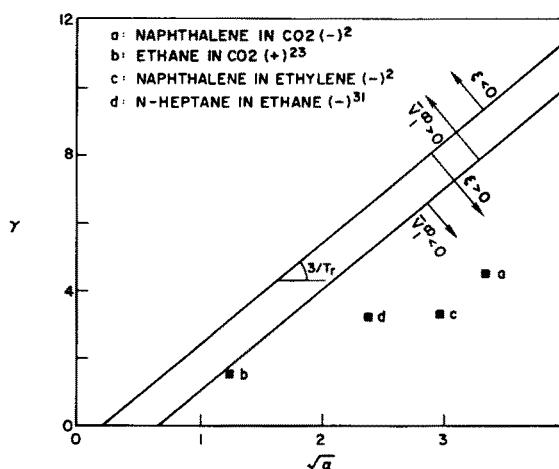

FIG. 2. The three possible types of behavior which characterize a near-critical van der Waals system. Attractive behavior occurs when $\gamma < 3\alpha^{1/2}/T_r - 2$; repulsive behavior, when $\gamma > 3\alpha^{1/2}/T_r - 2/3$ and weakly attractive behavior, when $3\alpha^{1/2}/T_r - 2 < \gamma < 3\alpha^{1/2}/T_r - 2/3$. The slope of the lines becomes $3(1 - k_{ij})/T_r$ upon introducing an interaction parameter k_{ij}, $a_{ij} = (1 - k_{ij})(a_{ii}a_{jj})^{1/2}$. Also shown are the $(\alpha^{1/2}, \gamma)$ coordinates pertaining to systems for which positive or negative divergence has been experimentally measured.

ancy in the ethane–carbon dioxide case (for which $\overline{V}_1 > 0$ has been measured at $T_r = 1.005$) merely reflects the inaccuracy of a purely van der Waals–Lorentz–Berthelot description of this system: upon introducing an interaction parameter k_{12} [i.e., $a_{12} = (1 - k_{12})(a_{11}a_{22})^{1/2}$] the slope of the plotted lines becomes $3(1 - k_{12})/T_r$, and the system becomes positively divergent at $T_r = 1$ for $k_{12} = 0.05$.

For $\rho \neq \rho_c$, Eqs. (12) and (13) read, with $\rho_r \equiv \rho/\rho_c$,

$$\overline{V}_1^\infty > 0 \quad \text{(i.e., } \delta > 0\text{)} \quad \text{for} \quad \gamma > \frac{3(3 - \rho_r)^2}{4} \cdot \frac{\alpha^{1/2}}{T_r} + 1 - \frac{3}{\rho_r}, \tag{16a}$$

$$\overline{V}_1^\infty < 0 \quad \text{(i.e., } \delta < 0\text{)} \quad \text{for} \quad \gamma < \frac{3(3 - \rho_r)^2}{4} \cdot \frac{\alpha^{1/2}}{T_r} + 1 - \frac{3}{\rho_r}, \tag{16b}$$

$$\xi > 0 \quad \text{(i.e., } \rho kT - \delta > 0\text{)} \quad \text{for}$$
$$\gamma < \frac{3(3 - \rho_r)^2}{4} \cdot \frac{\alpha^{1/2}}{T_r} + \left(\frac{\rho_r}{3} - 1\right), \tag{17a}$$

$$\xi < 0 \quad \text{(i.e., } \rho kT - \delta < 0\text{)} \quad \text{for}$$
$$\gamma > \frac{3(3 - \rho_r)^2}{4} \cdot \frac{\alpha^{1/2}}{T_r} + \left(\frac{\rho_r}{3} - 1\right). \tag{17b}$$

Since $(\rho_r/3 - 1) \geqslant (1 - 3/\rho_r)$ (the equal sign corresponding to $\rho_r = 3$) the above equations define the same regimes as Eqs. (12) and (13). The behavior of $\overline{V}_1^\infty$ and ξ for $\rho_r \ll 1$ and $\rho_r \approx 3$, as predicted by Eqs. (16) and (17) exhibits interesting features. These limits, however, are obviously beyond the near-critical region (the van der Waals equation is unphysical for $\rho_r > 3$). Since, furthermore, the very concept of a cluster size rapidly loses mechanistic significance outside of the near-critical region,[24] such predictions are beyond the scope of this paper. Here we focus instead on the behavior of systems for which ξ and $\overline{V}_1^\infty$ are both large. In this case, since both $\overline{V}_1^\infty$ and ξ scale as K_T, their ratio must be weakly dependent upon ρ for a given T,[24] and the value of this ratio at $\rho = \rho_c$ is indeed representative of the effects being quantified here.

In Eqs. (12), (13), (16), and (17), we have used the Lorentz–Berthelot combining rule, $a_{12} = (a_{11}a_{22})^{1/2}$. Since this is unnecessarily restrictive, we consider the general case $a_{12} \neq (a_{11}a_{22})^{1/2}$, $a = \Sigma\Sigma x_i x_j a_{ij}$. Equations (12), (13), (16), and (17) then apply unchanged, but with $\alpha^{1/2}$ replaced with α', where

$$\alpha' = a_{12}/a_{22}.$$

The regimes now read, along the critical isochore,

$$\overline{V}_1^\infty > 0 \quad \text{(i.e., } \delta > 0\text{)} \quad \text{for} \quad \gamma > \frac{3\alpha'}{T_r} - 2, \tag{18}$$

$$\overline{V}_1^\infty < 0 \quad \text{(i.e., } \delta < 0\text{)} \quad \text{for} \quad \gamma < \frac{3\alpha'}{T_r} - 2, \tag{19}$$

$$\xi > 0 \quad \text{(i.e., } \rho kT - \delta > 0\text{)} \quad \text{for} \quad \gamma < \frac{3\alpha'}{T_r} - \frac{2}{3}, \tag{20}$$

$$\xi < 0 \quad \text{(i.e., } \rho kT - \delta < 0\text{)} \quad \text{for} \quad \gamma > \frac{3\alpha'}{T_r} - \frac{2}{3}, \tag{21}$$

and, for $\rho \neq \rho_c$,

$$\overline{V}_1^\infty > 0 \quad \text{(i.e., } \delta > 0\text{)} \quad \text{for} \quad \gamma > \frac{3(3 - \rho_r)^2}{4} \cdot \frac{\alpha'}{T_r} + \left(1 - \frac{3}{\rho_r}\right), \tag{22}$$

$$\overline{V}_1^\infty < 0 \quad \text{(i.e., } \delta < 0\text{)} \quad \text{for} \quad \gamma < \frac{3(3 - \rho_r)^2}{4} \cdot \frac{\alpha'}{T_r} + \left(1 - \frac{3}{\rho_r}\right), \tag{23}$$

$$\xi > 0 \quad \text{(i.e., } \rho kT - \delta > 0\text{)} \quad \text{for}$$
$$\gamma < \frac{3(3 - \rho_r)^2}{4} \cdot \frac{\alpha'}{T_r} + \left(\frac{\rho_r}{3} - 1\right), \tag{24}$$

$$\xi < 0 \quad \text{(i.e., } \rho kT - \delta < 0\text{)} \quad \text{for}$$
$$\gamma > \frac{3(3 - \rho_r)^2}{4} \cdot \frac{\alpha'}{T_r} + \left(\frac{\rho_r}{3} - 1\right). \tag{25}$$

thus, even with a_{12} as a free parameter, we recover formally identical criteria provided we replace $\alpha^{1/2}$ with α'. Alternatively, we can define an interaction parameter k_{12}, $a_{12} = (1 - k_{12})(a_{11}a_{22})^{1/2}$, a form frequently used in engineering calculations to express deviations from Lorentz–Berthelot combining rules.[32] In this case, Eqs. (12), (13), (16), and (17) are unchanged in form, but $\alpha^{1/2}$ is replaced by $(1 - k_{12})\alpha^{1/2}$.

IMPLICATIONS OF THE CLASSIFICATION CRITERIA

Given any near-critical system, consider the "symmetric" mixture obtained by interchanging solute and solvent (i.e., the infinitely dilute solute becomes the near-critical solvent, and vice versa). The two models which we have chosen in order to illustrate near-critical behavior differ in an important way as to their predictions concerning the behavior of symmetric mixtures. In order to illustrate these differences, we consider, in the first place, a van der Waals mixture, and define

$$\omega = 1/\gamma, \tag{26}$$

$$\Lambda = 1/\alpha^{1/2}. \tag{27}$$

Assuming that the actual (α, γ) system is attractive, we have $\omega^{-1} < (3/\Lambda T_r) - 2$ or, equivalently,

$$\omega > \frac{\Lambda}{\dfrac{3}{T_r} - 2\Lambda}, \tag{28}$$

whereas, for the symmetric (Λ, ω) system to be attractive, we require

$$\omega < \frac{3\Lambda}{T_r} - 2. \tag{29}$$

Thus, in order for a given near-critical binary mixture and the symmetric system obtained by interchanging solute and solvent both to exhibit attractive behavior, Eqs. (28) and (29) must be satisfied simultaneously (note that T_r, though constant, represents different actual temperatures in the above equations, since the $1 \rightleftarrows 2$ transformation in which we are interested preserves the near criticality of the given system). Similarly, for repulsive behavior to be preserved under the $1 \rightleftarrows 2$ transformation, we require that

$$\omega < \cfrac{\Lambda}{\cfrac{3}{T_r} - \cfrac{2\Lambda}{3}} \qquad (30)$$

and simultaneously,

$$\omega > \frac{3\Lambda}{T_r} - \frac{2}{3}. \qquad (31)$$

In this way, we construct Fig. 3, where the attractive, weakly attractive, and repulsive regimes for the infinite set of all possible "given" (i.e., $\alpha^{1/2}, \gamma$) systems are bounded by $\omega = \omega(\Lambda)$ curves, whereas the corresponding regimes for the infinite set of all possible "symmetric" (i.e., Λ, ω) systems are bounded by straight lines identical to those shown in Fig. 2. If a mixture is such that its representative (Λ, ω) point lies on regions corresponding to the same behavior as defined by the curves *and* the straight lines, then the system and the symmetric near-critical binary obtained by interchanging solute and solvent exhibit the same behavior. As an example, consider point A (Fig. 3). Its coordinates are such that the given mixture is attractive (i.e., α and γ are such that point A, with coordinates $\alpha^{-1/2}$ and γ^{-1}, lies above curve a), while the "symmetric" mixture is repulsive (i.e., Λ and ω are such that point A lies above line b').

It follows from Fig. 3 that it is impossible for any van der Waals near-critical system and its symmetric counterpart both to exhibit attractive behavior, since lines a and a' are, at best, tangent ($T_r = 1$) and do not intersect for $1 < T_r < 3$ (i.e., they do not intersect in the near-critical region). The Λ axis, line b' and curve b define a small triangular region with coordinates $\{0;0\}$, $\{2T_r/9;0\}$, $\{(9/4T_r - 5T_r/36)$
$- [(5T_r/36 - 9/4T_r)^2 - 1]^{1/2}$; $(27/4T_r^2 - 13/2)$
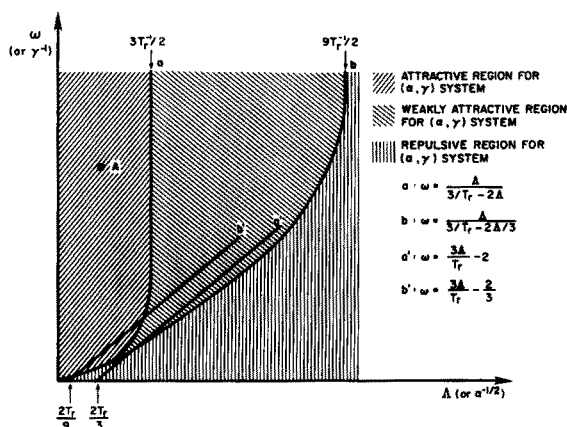$- [(15/36 - 27/4T_r^2)^2 - 9/T_r^2]^{1/2}\}$, shown in black in

FIG. 3. Attractive, weakly attractive and repulsive regions corresponding to a van der Waals near-critical system and to its symmetric counterpart obtained by interchanging solute and solvent. The behavior of a "given" system is described by the position of its representative point, in $(\alpha^{-1/2}, \gamma^{-1})$ coordinates, relative to curves a and b. The "symmetric" system is described by the position of the same point with respect to lines a' and b', as in Fig. 2. Point A represents an attractive "given" mixture whose "symmetric" counterpart is repulsive. If a "given" mixture's $(\alpha^{-1/2}, \gamma^{-1})$ coordinates fall within the black triangle, both the "given" and "symmetric" systems are repulsive. No "given"–"symmetric" pair is simultaneously attractive.

Fig. 3. This region is such that repulsive behavior in a given system implies repulsive behavior in its symmetric counterpart. It can be seen that weakly attractive behavior can, in principle, also be preserved under the $1 \rightleftharpoons 2$ transformation. In general, though, near-critical binaries and their symmetric counterparts are not predicted to exhibit the same behavior when modelled by the van der Waals equation.

If we consider a_{12} as a free parameter, we can write, as before, $a_{12} = (1 - k_{12})(a_{11}a_{22})^{1/2}$, whereupon we recover Eqs. (28)–(31), but with $3/T_r$ now replaced with $3(1 - k_{12})/T_r$, and ω, Λ still defined as per Eqs. (26) and (27). The two Λ intercepts and the slope of the a' and b' lines (Fig. 3) then become $2T_r/[3(1 - k_{12})]$, $2T_r/[9(1 - k_{12})]$, and $3(1 - k_{12})/T_r$; the vertical asymptotes of curves a and b become $3(1 - k_{12})/(2T_r)$ and $9(1 - k_{12})/2T_r$. The intersection of curve a and lie a', a necessary but not sufficient condition for a mixture and its symmetric counterpart both to exhibit attractive behavior, does not occur for $(1 - k_{12}) < T_r < 3(1 - k_{12})$. Thus, it becomes indeed possible for a van der Waals mixture and its symmetric counterpart both to exhibit attractive behavior, but this requires very large deviations in a_{12} away from its Lorentz–Berthelot value. As an example, in order for curve a and line a' to intersect for $T_r \geqslant 1.01$, it is necessary to have $k_{12} = 0.6633$. Since the interaction parameter should, in principle, be small compared to unity, a large k_{12} is generally indicative of the inaccuracy of the equation of state, rather than of the combining rule.

We now consider the behavior of a given mixture and its symmetric counterpart as predicted by Wheeler's model. Although in this model the solute does not have a critical point, the formalism can nevertheless be used as a model of near criticality by considering its infinitely dilute limit (with respect to the secondary lattice) exclusively, the primary lattice being near critical. Upon interchanging labels $(1 \rightleftharpoons 2)$, we go from the given near-critical system to its symmetrical near-critical counterpart. At the critical point of a cubic lattice, Eq. (9b) becomes

$$|\epsilon_{12}|/kT_c > 1.211. \qquad (32)$$

But, for such a lattice, $kT_c = 1.124|\epsilon|$ (where $\epsilon < 0$ is the solvent's attractive energy). Thus, for attractive behavior, we must have[33]

$$|\epsilon_{12}| > 1.361|\epsilon_{22}| \quad \text{for } \overline{V}_1^\infty \rightarrow -\infty \text{ as } x_1 \rightarrow 0 \qquad (33)$$

and, at the other end of the concentration range,

$$|\epsilon_{12}| > 1.361|\epsilon_{11}| \quad \text{for } \overline{V}_2^\infty \rightarrow -\infty \text{ as } x_1 \rightarrow 1. \qquad (34)$$

Thus, when we consider Wheeler's decorated lattice in the limit of infinite dilution with respect to the solute, and use this as a picture of near criticality at both ends of the composition range (that is to say, we obtain the near criticality of the symmetric system by switching labels while remaining at infinite dilution with respect to the secondary lattice and near criticality vis-à-vis the primary lattice), the model predicts the behavior shown in Table I, where we have used the fact that the sign of ϵ_{12} is unaffected by $1 \leftrightarrows 2$ interchange.

Note in particular, that a Lorentz-Berthelot constraint (i.e., $|\epsilon_{12}| = |\epsilon_{11}\epsilon_{22}|^{1/2}$) can imply weakly attractive $\leftrightarrows$

TABLE I. Behavior of a "given" ⇆ "symmetric" pair as predicted by Wheeler's model upon switching labels at infinite dilution and near-criticality.

ϵ_{12}	Eq. (33)	Eq. (34)	Given	Symmetric
>0	$\cdots$	$\cdots$	Repulsive	Repulsive
<0	Satisfied	Satisfied	Attractive	Attractive
<0	Satisfied	Violated	Attractive	Weakly attractive
<0	Violated	Satisfied	Weakly attractive	Attractive
<0	Violated	Violated	Weakly attractive	Weakly attractive

weakly attractive, attractive ⇆ weakly attractive, or repulsive ⇆ repulsive behavior.

The types of behavior shown in Table I are clearly at odds with van der Waals predictions: attractive ⇆ repulsive and weakly attractive ⇆ repulsive behavior are allowed in the van der Waals case and forbidden in Wheeler's model, whereas attractive behavior is almost never preserved in the former case (except for very high deviations in a_{12} from its Lorentz–Berthelot value), and easily preserved in the latter. Furthermore, repulsive behavior is necessarily preserved in Wheeler's model, and almost never preserved for a van der Waals mixture.

Although recent computer simulations of near-critical Lennard–Jonesiums[34] confirm the validity of the van der Waals picture, experimental investigations of partial molar volumes in near-critical mixtures and their symmetric counterparts are needed in order to clarify this interesting matter. It is clear, though, that neither model is adequate in the case of systems whose components differ greatly in size.

ENTROPY, ENTHALPY, AND VOLUME CHANGES

In the immediate vicinity of the critical point, the solute's partial molar enthalpy becomes proportional to its partial molar volume, with a positive proportionality constant related to the slope of the solvent's coexistence curve[10,24]

$$\frac{\bar{H}_1^\infty}{\bar{V}_1^\infty} \sim T\left(\frac{\partial P}{\partial T}\right)_\sigma \qquad (35)$$

or equivalently,

$$\frac{\bar{H}_1^\infty \xi^{-1}}{kT_c} \sim T_r Z_c \left(\frac{\partial P_r}{\partial T_r}\right)_\sigma \left(\frac{\rho_c}{\rho}\right) \frac{\delta}{\rho kT - \delta}, \qquad (36)$$

where subscript σ denotes the coexistence curve, $P_r = P/P_c$, and Z_c is the solvent's compressibility factor at the critical point. Along the critical isochore, therefore,

$$\frac{\bar{H}_1^\infty \xi^{-1}}{kT_c} \sim T_r Z_c \left(\frac{\partial P_r}{\partial T_r}\right)_\sigma \frac{\delta}{\rho_c kT - \delta} \equiv \psi. \qquad (37)$$

Note that because $\bar{V}_1^\infty$ and ξ are diverging quantities, reference enthalpies in Eqs. (35)–(37) vanish upon normalizing by $\bar{V}_1^\infty$ or ξ.

In strict analogy with Eq. (6), the quantity ψ is the enthalpy change associated with cluster formation (in units of kT_c) per excess solvent molecule surrounding the infinitely dilute solute, with respect to a uniform distribution at bulk conditions. It is obvious that ψ is a finite quantity (the special case $\rho_c kT \approx \delta$ will be discussed below), and that the di-

vergence criteria derived for $\bar{V}_1^\infty$ apply unmodified to $\bar{H}_1^\infty$. Note, however, that whereas Eqs. (5) and (6) are exact, Eqs. (36) and (37) are only asymptotically so.

We will now quantify the specific (i.e., normalized by ξ) volume, enthalpy and entropy changes which accompany the formation of solvent-rich ($\xi > 0$) or solvent-deficient regions ($\xi < 0$) around infinitely dilute solutes in near-critical systems. In the case of entropy, we must separate the ideal mixing term, which diverges at infinite dilution. The appropriate quantity in this case[24] is the excess partial molar entropy with respect to that of an infinitely dilute solute in an ideal gas mixture $(\bar{S}_1^\infty)_{igm}$ at the same temperature and density, but at a pressure $P_{igm} = \rho kT$,

$$[\bar{S}_1^\infty]^{ex} = \bar{S}_1^\infty - (\bar{S}_1^\infty)_{igm}$$

$$= -\int_0^P \left[\left(\frac{\partial \bar{V}_1^\infty}{\partial T}\right)_P - \frac{k}{P}\right] dP + k \ln \frac{\rho kT}{P} \qquad (38)$$

where k is Boltzmann's constant. $(\bar{S}_1^\infty)^{ex}$ diverges as $\bar{V}_1^\infty$ and $\bar{H}_1^\infty$, its sign being that of δ.[24] Thus, for negatively divergent systems, $(\bar{S}_1^\infty)^{ex}$ is a measure of the order brought about by long-ranged correlations around a central solute molecule which attracts solvent molecules. We thus see that the cooperative volume, enthalpy, and entropy effects, when normalized by ξ, are singularity-free quantities, which can be compared to the corresponding volume, enthalpy, and entropy changes which characterize the solvent's vapor–liquid transition. Because ϕ, ψ, and $(\bar{S}_1^\infty)^{ex} \xi^{-1}$ are singularity-free, and the pure component effects with which they will be compared are not, in general, restricted to the near-critical regime, we can define a van der Waals q parameter,

$$q = \left(1 + \frac{\gamma}{2}\right)\left(\frac{3\alpha^{1/2}}{2T_r}\right)^{-1} \qquad (39)$$

such that $\delta > 0$ for $q > 1$ and $\delta < 0$ for $q < 1$. Along the critical isochore of a van der Waals solvent, Eqs. (6) and (37) read

$$\phi = \frac{q - 1}{\dfrac{4T_r \alpha^{-1/2}}{9} - (q - 1)}, \qquad (40)$$

$$\psi = \frac{q - 1}{\dfrac{8\alpha^{-1/2}}{27} - \dfrac{2(q - 1)}{3T_r}}. \qquad (41)$$

Figure 4 shows the cooperative volume, enthalpy, and entropy changes along the critical isochore (normalized by ξ) which accompany the formation of solvent-rich and solvent-deficient regions containing, respectively, ξ and $(-\xi)$ excess solvent molecules, upon addition of trace amounts of a solute to the near-critical solvent. Because α and T_r are fixed, changes in q correspond to changes in γ (solute/solvent volume ratio in a van der Waals formulation). For $q < 1$ [or, in lattice terminology, $\epsilon_{12}/kT < -\ln(1 + N_c^{-1/2})$], ξ is positive, while $\bar{V}_1^\infty$, $\bar{H}_1^\infty$, and $(\bar{S}_1^\infty)^{ex}$ are all negative. The x axis then gives the reduced temperature at which the specific volume, enthalpy, and entropy changes of condensation associated with the van der Waals solvent's vapor–liquid transition equal $\bar{V}_1^\infty \xi^{-1}$, $\bar{H}_1^\infty \xi^{-1}$, and $(\bar{S}_1^\infty)^{ex} \xi^{-1}$, respectively. Likewise, for $q > 1 + 4T_r/9\alpha^{1/2}$ (or, in lattice termin-
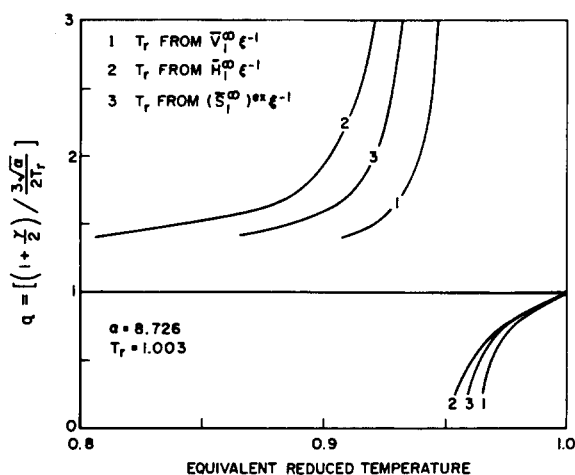
FIG. 4. Cooperative volume, enthalpy, and entropy changes associated with the formation of solvent-rich ($q < 1$) and solvent-lean regions around trace solute molecules in a near-critical van der Waals solvent. q is an asymmetry parameter. The x axis is the reduced temperature at which the volume, enthalpy, and entropy changes per molecule associated with the solvent's vapor–liquid transition equal $\overline{V}_1^\infty \xi^{-1}$, $\overline{H}_1^\infty \xi^{-1}$, and $(\overline{S}_1^\infty)^{\text{ex}} \xi^{-1}$, respectively. For $q < 1$ (attractive behavior; $\overline{V}_1^\infty < 0$, $\xi > 0$), the cooperative phenomenon is analogous to an induced condensation. For $q > 1 + 4T_r/9\alpha^{1/2}$ (repulsive behavior; $\overline{V}_1^\infty > 0$, $\xi < 0$), the cooperative phenomenon is analogous to an induced evaporation.

ology, $\epsilon_{12} > 0$) ξ is negative, while $\overline{V}_1^\infty$, $\overline{H}_1^\infty$, and $(\overline{S}_1^\infty)^{\text{ex}}$ are all positive. The x axis then gives the reduced temperature at which the specific volume, enthalpy, and entropy changes of vaporization associated with the van der Waals solvent's liquid–vapor transition equal $\overline{V}_1^\infty \xi^{-1}$, $\overline{H}_1^\infty \xi^{-1}$, and $(\overline{S}_1^\infty)^{\text{ex}} \xi^{-1}$, respectively. Technical details pertaining to the calculations performed in order to obtain Fig. 4 are discussed in the Appendix.

For $q < 1$ (attractive systems), γ increases monotonically along each of the three curves, from the infinitely small solute limit ($q = 0.226$ at the given α, T_r values) to the $q = 1$ limit. The closeness of the volume, enthalpy, and entropy curves suggests that clustering can be qualitatively described in terms of an induced phase transition in which the diverging correlation length causes a "condensation" of an arbitrarily large number of solvent molecules around the infinitely dilute solute. Of course, in a true phase transition, one would have a single curve instead of three.

For $q > 1 + 4T_r/9\alpha^{1/2}$ (ϵ_{12} repulsive in lattice terminology) ξ becomes arbitrarily large and negative. This implies that the infinitely dilute solute is surrounded by a region whose characteristic size is the correlation length, within which solvent concentration is less than in the bulk. Note that both in the "condensation" and "evaporation" cases, the cooperative phenomena involve entropic and energetic effects that are invariably greater in magnitude (lower equivalent T_r) than those which would accompany a vapor–liquid transition involving a volume change (per molecule) of $\overline{V}_1^\infty \xi^{-1}$.

For weakly attractive behavior [$1 < q < 1 + 4T_r/9\alpha^{1/2}$ or, in lattice terminology, $-\ln(1 + N_c^{-1/2}) < \epsilon_{12}/kT < 0$], the volume integral of ($g_{21}^\infty - 1$) diverges to $+\infty$ (clustering) but so do $\overline{V}_1^\infty$, $\overline{H}_1^\infty$, and $(\overline{S}_1^\infty)^{\text{ex}}$. Partial molar volume

measurements[23] and ξ calculations[8] based on these experiments indicate that the ethane(1)–CO_2(2) system exhibits this type of behavior. Clearly, spectroscopic studies of weakly attractive near-critical binaries would be extremely helpful in improving our mechanistic understanding of this class of systems.

When γ is close to $3\alpha^{1/2}/T_r - 2/3$ (i.e., $\rho k T \approx \delta$, or, in lattice terminology, when ϵ_{12} is close to 0), systems exhibit large positive $\overline{V}_1^\infty$, $\overline{H}_1^\infty$, and $(\overline{S}_1^\infty)^{\text{ex}}$ but (except for the immediate vicinity of the critical point) small ξ, which can be either positive or negative. In this case, ψ and ϕ become arbitrarily large. We are not aware of any system exhibiting this behavior.

CONCLUSION

The presence of trace amounts of a solute within a near-critical solvent gives rise to cooperative phenomena which can be described with qualitative accuracy as induced phase transitions. The magnitude of the cooperative volume, enthalpy and entropy changes per solvent molecule are comparable to the corresponding condensation and evaporation effects associated with the solvent's vapor–liquid phase transition.

In an attractive near-critical mixture, an arbitrarily large solvent-rich region is formed around the solute, giving rise to negatively diverging solute partial molar volumes. If, on the other hand, solute–solvent interactions are repulsive, an arbitrarily large solvent-deficient region is formed around the solute, and its partial molar volume diverges to $+\infty$. In the case of weakly attractive mixtures, positively diverging solute partial molar volumes coexist with positively correlated solute–solvent concentration fluctuations.

We have analyzed the three types of behavior with two very different models: Wheeler's decorated lattice, a microscopic model originally developed to study near-critical binary mixtures taking into account nonclassical effects, and the van der Waals model, a continuum and classical picture. In the former case, the attractive, weakly attractive, and repulsive regimes are obtained from energetic considerations exclusively. By contrast, in the van der Waals case, the same regimes follow from molecular size and energy considerations. This leads to conflicting predictions regarding the behavior of the symmetric near-critical system obtained by interchanging the roles of infinitely dilute solute and near-critical solvent, which can only be reconciled by allowing very high deviations in the van der Waals a_{12} parameter away from its Lorentz–Berthelot value.

Experimental measurements of infinite dilution partial molar volumes in near-critical systems and their symmetric counterparts will provide valuable information on the relative merits of decorated lattice and van der Waals predictions. In addition, spectroscopic studies of weakly attractive and repulsive systems, coupled with partial molar volume measurements, will shed light on the interesting behavior of mixtures in which positive solute–solvent concentration fluctuation correlations coexist with positively divergent solute partial molar volumes, and on mixtures in which large

solvent-deficient regions are formed around each solute molecule, respectively.

Theoretically, it is necessary to investigate the predictions of other microscopic and nonclassical models[22] with respect to the behavior of symmetric near-critical mixtures obtained by $1 \leftrightarrows 2$ interchange, and to study near-critical mixtures in which the solute is much larger than the solvent, a situation encountered in polymer–supercritical fluid systems.[27,28]

ACKNOWLEDGMENTS

The authors gratefully acknowledge the financial support of the National Science Foundation (Presidential Young Investigator Award CBT-8657010 to P.G.D.) and of Merck, Sharp and Dohme Research Laboratories. P.G.D. wishes to thank Dr. Wu-Cheng Cheng, of W. R. Grace & Co., for asking an insightful question: the (belated) answer is Fig. 4.

APPENDIX

We first derive Eqs. (9) and (10) from Eq. (7). The denominator in Eq. (7) is the infinite dilution limit of the solute's activity coefficient,[10] and is therefore a positive quantity. For $\partial N'/\partial \rho \sim 0$ and $N' \to N_c$, Eqs. (9a) and (9b) follow trivially. As for Eq. (10), we write

$$\rho kT - \delta = \rho^2 kT \left[\frac{(x^2 - 1) - (x - 1)^2 (\partial N'/\partial \rho)}{1 + (x^2 - 1)\rho - N'(x - 1)^2} \right], \quad (A1)$$

where ρ, as explained before, is now dimensionless, and δ has units of energy. Since the denominator in Eq. (A1) is positive in the near-critical region, $\rho kT - \delta$ is positive for $x > 1$ and negative otherwise, from which Eqs. (10a) and (10b) follow. Note that, as long as $|\partial N'/\partial \rho| < 1$, the numerator's only physically meaningful root (i.e., $x \geqslant 0$) is $x = 1$, which implies that (10a) and (10b) are rigorously true in the near-critical region.

It is straightforward to show that Eqs. (10a) and (10b) can also be obtained from Wheeler's decorated lattice model by direct calculation of the quantity $\langle \delta N_1 \delta N_2 \rangle / \langle N_1 \rangle$ at infinite dilution [see Eq. (3)]. This involves calculating the mixed second derivative of the grand partition function with respect to the logarithms of solute and solvent activities to obtain, at infinite dilution

$$\xi = \lim_{x_1 \to 0} \frac{\langle \delta N_1 \delta N_2 \rangle}{\langle N_1 \rangle}$$

$$= \frac{\rho^2 kTK_T [(x^2 - 1) - (x - 1)^2 (\partial N'/\partial \rho)_T]}{1 + \rho(x^2 - 1) - N'(x - 1)^2}$$

from which (10a) and (10b) follow (in the above equation, K_T is now the solvent's compressibility divided by the unit volume of a primary cell, since ρ is dimensionless).

In order to obtain Fig. 4, ϕ was calculated from Eq. (37), and the equivalent reduced temperature was obtained by finding the subcritical temperature at which the volume changes associated with condensation ($q < 1$) or evaporation of the van der Waals fluid equal $\overline{V}_1^\infty \xi^{-1}$. The coexistence curve, as well as the associated volume, enthalpy and entropy changes for the van der Waals fluid are all, of course,

amenable to explicit calculation. In the case of enthalpy, results obtained from Eq. (41) were indistinguishable from those obtainable by computing $\overline{H}_1^\infty$ explicitly,[24] as

$$\overline{H}_1^\infty = \frac{5kT}{2} + \int_0^P \left[\overline{V}_1^\infty - T \left(\frac{\partial \overline{V}_1^\infty}{\partial T} \right)_P \right] dP \qquad (A2)$$

and dividing by ξ, both quantities calculated along the critical isochore of the van der Waals fluid, which satisfies $T_r = (P_r + 3)/4$. In this approach, each point along a curve in Fig. 4 implies an integral of the type shown in (A2), with γ computed from the given α, T_r, and q, and an upper limit of integration such that $P_r = 4T_r - 3$. The integrals were obtained from the van der Waals equation, with no interaction parameter and van der Waals 1 mixing rules.[24] As explained before [see text immediately following Eq. (37)] the quantity $5kT/2$ vanishes upon division by ξ, since the latter is arbitrarily large close to criticality. In order to obtain the equivalent reduced temperature, the condensation ($q < 1$) and evaporation enthalpy changes associated with the van der Waals fluid's vapor–liquid transition were compared with $\overline{H}_1^\infty \xi^{-1}$.

Similarly, for entropy calculations, the van der Waals equation with van der Waals 1 mixing rules and zero interaction parameter[24] was used to compute Eq. (38), with γ computed from the given α, T_r, and q, and an upper limit of integration such that $P_r = 4T_r - 3$. In order to obtain the equivalent reduced temperature, the condensation ($q < 1$) and evaporation entropy changes associated with the van der Waals fluid's vapor–liquid transition were compared with $(\overline{S}_1^\infty)^{\text{ex}} \xi^{-1}$.

[1] C. A. Eckert, D. H. Ziger, K. P. Johnston, and T. K. Ellison, Fluid Phase Equil. **14**, 167 (1983).
[2] C. A. Eckert, D. H. Ziger, K. P. Johnston, and S. Kim, J. Phys. Chem. **90**, 2738 (1986).
[3] S. W. Kim and K. P. Johnston, Ind. Eng. Chem. Res. **26**, 1206 (1987).
[4] S. W. Kim and K. P. Johnston, AIChE J. **33**, 1603 (1987).
[5] S. Kim, J. M. Wong, and K. P. Johnston, in *Supercritical Fluid Technology*, edited by J. M. L. Penninger, M. Radosz, M. Mc Hugh, and V. J. Krukonis (Elsevier, Amsterdam, 1985).
[6] A. M. Rozen, Russ J. Phys. Chem. **50**, 837 (1976).
[7] G. Morrison, J. M. H. Levelt Sengers, R. F. Chang, and J. J. Christensen, in *Supercritical Fluid Technology*, edited by J. M. L. Penninger, M. Radosz, M. Mc Hugh, and V. J. Krukonis (Elsevier, Amsterdam, 1985).
[8] P. G. Debenedetti, Chem. Eng. Sci. **42**, 2203 (1987).
[9] I. R. Krichevskii, Russ. J. Phys. Chem. **41**, 1332 (1967).
[10] J. C. Wheeler, Ber. Bunsenges. Phys. Chem. **76**, 308 (1972).
[11] B. Widom, J. Chem. Phys. **46**, 3324 (1967).
[12] R. K. Clark, J. Chem. Phys. **48**, 741 (1968).
[13] G. Neece, J. Chem. Phys. **47**, 4112 (1967).
[14] J. M. H. Levelt Sengers, Fluid Phase Equil. **30**, 31 (1986).
[15] J. M. H. Levelt Sengers, G. Morrison, and R. F. Chang, Fluid Phase Equil. **14**, 19 (1983).
[16] J. M. H. Levelt Sengers, G. Morrison, G. Nielson, R. F. Chang, and C. M. Everhart, Int. J. Thermophys. **7**, 231 (1986).
[17] J. M. H. Levelt Sengers, R. F. Chang, and G. Morrison, in *Equations of State: Theories and Applications*, edited by K. C. Chao and R. L. Robinson [Am. Chem. Soc. Symp. Ser. No. 300, 110 (1986)].
[18] R. F. Chang and J. M. H. Levelt Sengers, J. Phys. Chem. **90**, 5921 (1986).
[19] R. F. Chang, G. Morrison, and J. M. H. Levelt Sengers, J. Phys. Chem. **88**, 3389 (1984).
[20] J. V. Sengers and J. M. H. Levelt Sengers, Ann. Rev. Phys. Chem. **37**, 189 (1986).
[21] G. C. Nielson and J. M. H. Levelt Sengers, J. Phys. Chem. **91**, 4078 (1987).
[22] S. W. Gilbert and C. A. Eckert, Fluid Phase Equil. **30**, 41 (1986).

[23]N. E. Khazonova and E. E. Sominskaya, Russ. J. Phys. Chem. **42**, 676 (1968).

[24]P. G. Debenedetti and S. K. Kumar, AIChE J. **34**, 645 (1988).

[25]W. Rozelius, O. Vizthum, and P. Hubert, U.S. Patent No. 3 843 824 (1974).

[26]T. M. Doscher and M. El-Arabi, Oil Gas J. **80**, 144 (1982).

[27]S. K. Kumar, Sc.D. thesis, Massachusetts Institute of Technology, Cambridge, 1986.

[28]S. K. Kumar, U. W. Suter, and R. C. Reid, Fluid Phase Equil. **29**, 373 (1986).

[29]J. G. Kirkwood and F. P. Buff, J. Chem. Phys. **19**, 774 (1951).

[30]We are grateful for suggestions on an interpretation of weakly attractive mixtures starting from the $\xi \to 0$ limit.

[31]P. C. Wu and P. Ehrlich, AIChE J. **19**, 533 (1973).

[32]J. M. Prausnitz, R. N. Liechtenthaler, and E. G. de Azevedo, *Molecular Thermodynamics of Fluid-Phase Equilibria*, 2nd ed. (Prentice-Hall, Englewood Cliffs, N.J., 1986), Chaps. 8 and 10.

[33]We are grateful for suggestions on the use of the solvent–solvent interaction as a second energy parameter in this context.

[34]I. Petsche and P. G. Debenedetti (in preparation).